
Beyond Single-Sample: Reliable Multi-Sample Distillation for Video Understanding

Songlin Li

University of Electronic Science and Technology of China
& Robotics Center, XPeng Motors
bigman2243197885@gmail.com

Xin Zhu*

Robotics Center, XPeng Motors
zhux9@xiaopeng.com

Zechao Guan

Robotics Center, XPeng Motors
guanzc2@xiaopeng.com

Peipeng Chen

Robotics Center, XPeng Motors
chenpp2@xiaopeng.com

Jian Yao

Robotics Center, XPeng Motors
jian.yao@xiaopeng.com

Abstract

Traditional black-box distillation for Large Vision-Language Models (LVLMs) typically relies on a single teacher response per input, which often yields high-variance responses and format inconsistencies in multimodal or temporal scenarios. To mitigate this unreliable supervision, we propose *R-MSD* (Reliable Multi-Sample Distillation), a framework that explicitly models teacher sampling variance to enhance distillation stability. Rather than relying on a single teacher response, our approach leverages a task-adaptive teacher pool to provide robust supervision tailored to both closed-ended and open-ended reasoning. By integrating quality-aware signal matching with an adversarial distillation objective, our approach effectively filters teacher noise while maximizing knowledge transfer. Extensive evaluations across comprehensive video understanding benchmarks demonstrate that *R-MSD* consistently outperforms single sample distillation methods. We additionally include an original SFT+RL 4B baseline under the same training budget, which shows only marginal gains, while our method achieves significant improvements. With a 4B student model, our approach delivers gains on VideoMME (+1.5%), Video-MMMU (+3.2%), and MathVerse (+3.6%).

1 Introduction

Large Vision-Language Models (LVLMs) [Chen et al., 2024a, Li et al., 2025a, Guo et al., 2025a] have advanced video understanding, but deployment is hindered by computational costs. To address this challenge, knowledge distillation [Hinton et al., 2015] transfers knowledge from a strong teacher to a smaller student. Recent analysis [Yue et al., 2025] shows that distillation can expand a model’s reasoning capabilities beyond what reinforcement learning achieves, as RL methods are bounded by the base model’s distribution. While prior work explores multi-teacher aggregation [You et al., 2017], cross-modal transfer [Mansourian et al., 2025], and adversarial objectives [Ye et al., 2025], these overlook a fundamental question: *is a single teacher sample reliable?*

*Corresponding Author

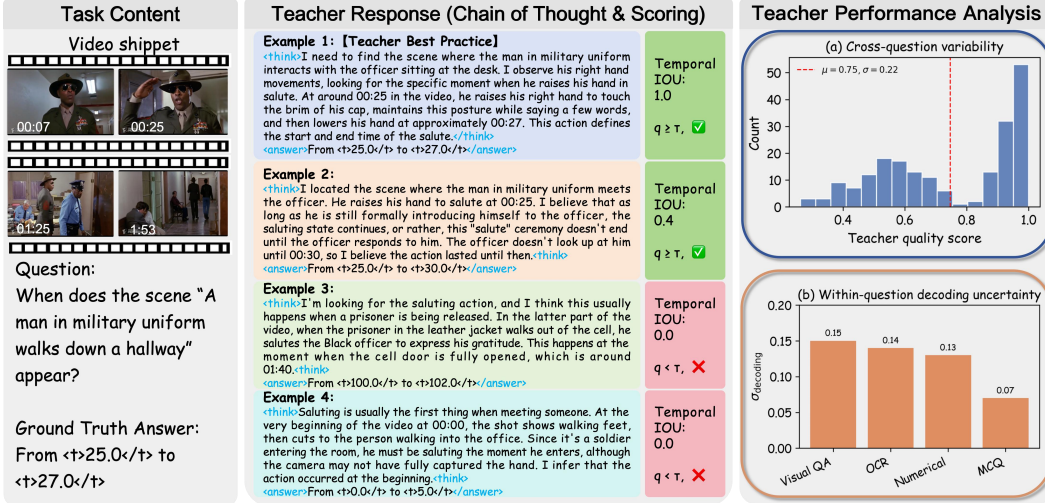


Figure 1: Teacher sampling variance in video understanding. **Left:** Temporal QA example: four teacher responses with their temporal IoU to ground truth, showing substantial quality variation across samples of the same question. **Right:** Global statistics over 200 teacher responses from eight task types: (a) cross-question variance and (b) within-question sampling variance. Both dimensions undermine single-sample distillation and motivate our multi-sample approach.

Existing distillation methods—from sequence-level imitation [Kim and Rush, 2016] to adversarial training [Ye et al., 2025]—typically assume that a single sampled teacher response per training input provides reliable supervision. In text-only settings, this assumption can be acceptable when stochastic decoding is relatively stable. In video understanding, we observe a different regime with *two dimensions of variance*, as illustrated in Figure 1. First, **cross-question variance** is substantial: quality spans $[0.10, 1.0]$ ($\mu=0.75, \sigma=0.22$) across 200 samples. MCQ shows high consistency ($\mu=0.96, \sigma=0.10$), while visual QA is variable ($\mu=0.64, \sigma=0.24$). Second, **within-question uncertainty** is also substantial: repeated sampling yields σ_{sampling} ranging from 0.07 (MCQ) to 0.15 (visual QA), with quality ranges of $[0.50, 0.85]$ for OCR and $[0.65, 1.00]$ for numerical tasks. Format violations occur in 1% of samples overall (10% for temporal QA).

Teacher-sampling variance interacts with task heterogeneity. Video benchmarks mix *closed-ended tasks* (verifiable outputs: temporal segments, bounding boxes, MCQ) and *open-ended tasks* (natural language). Closed-ended tasks allow quality-based filtering via ground-truth; open-ended tasks lack reliable metrics due to lexical-overlap penalties for semantically equivalent responses. Most distillation pipelines [Dou et al., 2025] apply uniform supervision and do not model this asymmetry.

To tackle the challenge of unreliable teacher sampling, we propose **R-MSD (Reliable Multi-Sample Distillation)**. The core idea is to sample a *teacher pool* of K responses per input and use task-adaptive quality signals to *bias which teacher responses are used for optimization*. Our training pipeline has two stages: Stage 1 performs SFT warmup on one selected teacher response per input; Stage 2 performs RL-based adversarial distillation, where the student generates multiple responses and each rollout is paired with one teacher response from the pool. For closed-ended tasks, teacher responses are preferentially paired based on ground-truth-based quality signals (e.g., temporal/spatial IoU or exact match, together with format validity checks), so higher-quality teachers are sampled more often. For open-ended tasks, we use uniform pairing to avoid brittle lexical ranking. We jointly train a discriminator (critic) on these paired student–teacher responses to provide distribution-level supervision alongside ground-truth-based rule rewards.

Our main contributions are:

- **Quantitative analysis of teacher decoding uncertainty.** We identify *teacher decoding uncertainty* as a central source of supervision noise in video LVLm distillation. Across 200 samples, quality varies substantially ($\sigma=0.22$ globally, up to $\sigma=0.29$ by task), and format violations are non-negligible (1.0% overall, 3.5% task-specific), showing that single-sample supervision is unreliable.

- **Method: R-MSD (Reliable Multi-Sample Distillation).** We propose a two-stage framework with a teacher pool per input and task-adaptive matching: quality-biased pairing for closed-ended tasks and uniform pairing for open-ended tasks. Combined with an online critic-as-discriminator, this improves supervision *quality*, not just supervision *quantity*.
- **Comprehensive validation.** We evaluate R-MSD on six video and two image QA benchmarks, demonstrating strong cross-domain transfer. Under the same test-time frame count, our distilled 4B student surpasses Qwen3-VL-4B on VideoMME (65.3 vs. 63.8), VideoMMMU (58.6 vs. 55.4), and WorldSense (49.2 vs. 46.7). An SFT+RL 4B baseline trained under a matched protocol yields only marginal gains compared with our task-adaptive multi-sample distillation.

2 Related Work

2.1 Video Understanding with Vision-Language Models

In the video domain, image LVLMs are extended with video-aware encoders, temporal tokenization, and video-instruction data. Representative systems include VideoChat/VideoChatGPT for conversational reasoning [Li et al., 2025b, Maaz et al., 2024], Video-LLaVA for unified image–video representations [Lin et al., 2024], and efficiency-oriented adaptations such as LLaMA-VID and PLLaVA [Li et al., 2024a, Xu et al., 2024]. Recent pipelines also improve data scale/quality via synthetic instruction and captioning refinement [Zhang et al., 2024, Chen et al., 2024b].

The central open issue is no longer whether LVLMs can follow video instructions, but how to optimize generation quality when outputs are open-ended and evaluation signals are noisy. Although supervised fine-tuning (SFT) is a strong baseline, open-ended video understanding often requires optimization beyond maximum-likelihood training. This motivates preference learning and reinforcement learning (RL) for direct quality optimization. In language modeling, RLHF [Ouyang et al., 2022] and direct alignment methods such as DPO [Rafailov et al., 2023] have become standard tools for quality optimization. Analogously, multimodal alignment has explored using large (multi)modal models as judges or feedback providers [Wang et al., 2024, Zhu et al., 2025a]. However, reward design for open-ended answers remains a central bottleneck: scalar rewards can be noisy, and learned reward models may be exploited by the policy during optimization (reward hacking) [Gao et al., 2023]. Recent analysis [Yue et al., 2025] shows that reinforcement learning with verifiable rewards (RLVR) improves sampling efficiency but does not expand reasoning capabilities beyond the base model’s distribution—whereas distillation can transfer genuinely new reasoning patterns from a stronger teacher.

Our work addresses a complementary reliability issue that appears *before* reward modeling: with few sampled teacher responses, the supervision signal itself can be unstable. Instead of relying on a fixed, offline-trained multimodal reward model as a judge (which can be vulnerable to reward hacking as the policy improves), we adopt an *adversarial distillation* perspective where the reward/critic is trained *online* alongside the student. This co-evolution provides adaptive supervision for open-ended video responses and reduces reliance on a static reward proxy that may become brittle as the policy improves.

2.2 Knowledge Distillation for Sequence Generation

Knowledge distillation (KD) transfers knowledge from a large teacher to a smaller student. Classic KD matches softened logits [Hinton et al., 2015], while modern compression techniques have been widely applied to Transformer architectures. For sequence generation, sequence-level distillation trains a student on teacher-generated outputs to reduce exposure bias [Kim and Rush, 2016]. With the rise of instruction-tuned LLMs, distillation has become a standard approach for creating smaller, capable assistants.

A key practical challenge is that many high-performing teachers are *black boxes* (accessible only via an API), making logit-based KD infeasible. This motivates response-based distillation methods that learn only from sampled teacher responses. Recently, Generative Adversarial Distillation (GAD) formulates black-box, on-policy distillation as a minimax game where a discriminator distinguishes student outputs from teacher outputs and serves as an online reward signal [Ye et al., 2025]. Concurrently, reward modeling has been re-interpreted as training policy discriminators,

e.g., POLAR, which learns a general reward model by discriminating policies rather than predicting absolute preference scores [Dou et al., 2025]. Recent OPD analysis further connects on-policy distillation to KL-constrained RL and studies reward-scaling and reference-model choices in a generalized formulation [Yang et al., 2026]. In this paper, we use *on-policy distillation* to denote this distillation paradigm in prior work (online sample generation with discriminator/reward co-training), which is distinct from the RL taxonomy term *on-policy RL*.

Two complementary trends in response-based distillation. Existing methods can be organized into two trends. The first is *supervised-style distillation*: sequence-level imitation, multi-sample filtering, and quality-aware selection [Kim and Rush, 2016, Wang et al., 2022, Zhou et al., 2023, Dong et al., 2023]. The second is *RL/adversarial-style distillation*: on-policy discriminator/reward training for distribution-level alignment [Ye et al., 2025, Dou et al., 2025, Yang et al., 2026]. R-MSD unifies these trends: it extends supervised-style distillation with task-adaptive quality weighting, while preserving online distribution-level alignment via adversarial objectives.

Multi-sample and quality-aware distillation. A natural extension of single-sample distillation is to use multiple teacher outputs per input. Multi-teacher distillation aggregates knowledge from diverse teachers [You et al., 2017, Fukuda et al., 2017], while self-ensemble methods generate multiple outputs from a single teacher to improve robustness [Wang et al., 2022]. Recent work has also explored quality-aware selection strategies, such as filtering low-quality samples based on confidence scores [Zhou et al., 2023] or using reward models to rank teacher outputs [Dong et al., 2023]. However, these approaches are primarily developed for text-only tasks and rely on logit-based signals or text-specific quality metrics. In the video domain, quality assessment must account for closed-ended outputs (e.g., temporal segments) and the unreliability of lexical metrics for open-ended responses—a distinction largely overlooked by prior work. While these advances are promising, existing black-box adversarial distillation methods are primarily developed and evaluated in *pure-text* settings. Extending them to video LLMs is challenging due to (i) a larger and noisier observation space, (ii) sensitivity to temporal sampling and grounding, and (iii) higher output-format heterogeneity across benchmarks. Multi-sample and multi-teacher distillation has been explored to use diverse teachers or generations, but many approaches emphasize teacher diversity rather than the stability of sampled supervision from a single strong teacher.

Our method builds on GAD-style online adversarial distillation and extends it to video-specific supervision noise. The key difference is explicit modeling of teacher decoding uncertainty with task-adaptive matching: ground-truth-informed quality estimation for closed-ended tasks and uniform treatment for open-ended supervision. This design reduces reliance on brittle lexical proxies while preserving online distribution-level alignment through an adaptive discriminator.

Overall, prior work leaves two gaps most relevant to our setting: (i) robust quality handling for open-ended video responses, and (ii) explicit modeling of supervision noise induced by teacher sampling. Our framework targets both by coupling R-MSD-style task-adaptive multi-sample supervision with online adversarial alignment.

3 Method

3.1 Problem Formulation

Given a video-question-answer tuple (V, Q, y^*) , our goal is to train a student model π_S from a stronger teacher π_T under black-box access. Unlike conventional sequence-level distillation that uses a single teacher sample, we model teacher sampling variance by drawing K teacher responses for the same input:

$$\{T_1, \dots, T_K\} \sim \pi_T(\cdot \mid V, Q). \tag{1}$$

Our objective is to convert this multi-sample set into a stable supervision signal that emphasizes reliable responses when correctness is verifiable and avoids lexical bias when correctness is not reliably measurable.

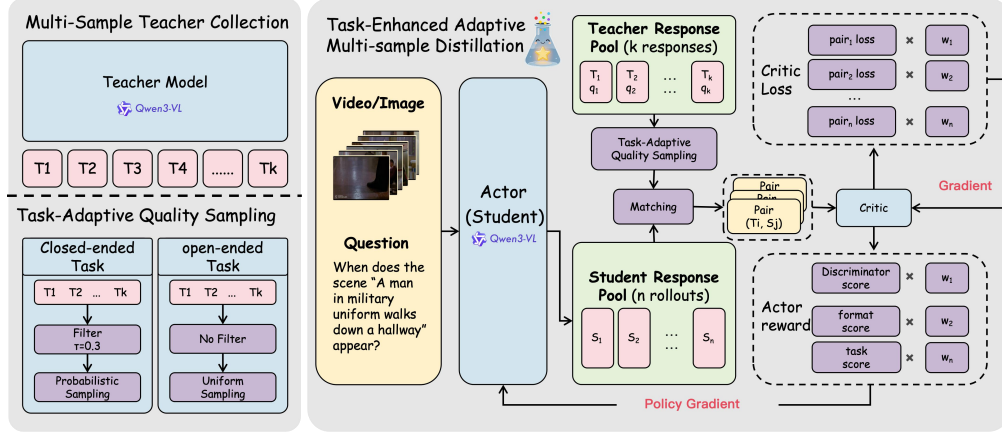


Figure 2: Overview of the R-MSD framework (Stage 2: RL-based Adversarial Distillation). The pipeline utilizes a multi-sample teacher collection to provide diverse references. A critic-as-discriminator mechanism is employed to perform task-adaptive sampling, matching student rollouts with teacher responses. The student policy is then iteratively refined through adversarial distillation, using a weighted combination of discriminator, format, and task-specific scores as the reward signal.

3.2 Overall Framework

Figure 2 illustrates **R-MSD** (Reliable Multi-Sample Distillation), which has three components: (1) *multi-sample teacher collection* (sample K teacher outputs per input), (2) *task-adaptive quality assessment* (GT-based scoring for closed-ended tasks, uniform weighting for open-ended tasks), and (3) *task-adaptive matching with online discrimination* (quality-aware pairing with a critic-as-discriminator). Training proceeds in two stages: **Stage 1** (SFT warmup) and **Stage 2** (RL-based adversarial distillation).

3.3 Task-Adaptive Quality Assessment and Matching

Task taxonomy. We classify tasks based on answer verifiability. *Closed-ended tasks* have answers that can be objectively verified against ground-truth annotations (e.g., temporal/spatial grounding, multiple-choice, binary QA, numerical regression, OCR). *Open-ended tasks* require open-ended natural language descriptions (e.g., detailed visual event description) where no generally reliable correctness metric exists.

3.3.1 Quality scoring for closed-ended tasks

For closed-ended tasks, we assign each teacher response T_k a ground-truth-based quality score $q_k \in [0, 1]$:

$$q_k = \mathbb{I}(\text{valid}(T_k)) \cdot \text{Metric}(T_k, y^*), \quad (2)$$

where $\mathbb{I}(\text{valid}(T_k))$ indicates format validity and $\text{Metric}(\cdot)$ is the task-specific metric. For MCQ tasks, the metric uses exact match: $q_k = 1$ if the predicted answer option matches the ground-truth option, and $q_k = 0$ otherwise. For temporal grounding we use temporal IoU; for spatial grounding we use IoU; for numerical tasks we use ϵ -accuracy. Unparseable or format-invalid responses receive $q_k = 0$. Samples with $q_k = 0$ remain in the teacher pool but have $p_k = 0$, meaning they are never selected during matching. For closed-ended tasks, we optionally apply quality filtering by setting $p_k = 0$ for teacher samples with $q_k < \tau$, where τ is a quality threshold (we use $\tau = 0.3$ in experiments, validated via sensitivity analysis in Table 4).

3.3.2 Uniform treatment for open-ended tasks

For open-ended tasks, we avoid lexical-overlap-based ranking by default to prevent false negatives from synonym/paraphrase variations. We therefore use uniform matching for this task family, setting $p_k = 1/K$ in Eq. 3.

3.3.3 Quality-weighted matching

Our implementation realizes “quality weighting” in Stage 2 via *quality-weighted matching* between multiple student rollouts and a teacher pool. For each input (V, Q) , we maintain a teacher pool $\{T_1, \dots, T_K\}$. During on-policy optimization, the student samples N responses $\{S_1, \dots, S_N\}$ for the same prompt. We then match each S_i to one teacher response $T_{m(i)}$:

$$m(i) \sim \text{Categorical}(p_1, \dots, p_K), \tag{3}$$

where the sampling distribution is task-adaptive. For closed-ended tasks,

$$p_k = \frac{q_k}{\sum_{j=1}^K q_j}, \tag{4}$$

after applying quality filtering ($q_k = 0$ for filtered samples). Higher-quality teacher samples are more likely to be paired and may be selected multiple times. For open-ended tasks, we use uniform matching $p_k = 1/K$. The matching probability p_k determines which teacher response $T_{m(i)}$ supervises each student rollout S_i in Stage 2. This avoids two failure modes: treating all closed-ended responses equally despite quality gaps, and over-penalizing open-ended responses with unreliable lexical metrics. Consequently, our method improves the reliability of supervision rather than merely increasing the number of training samples.

3.4 Two-Stage Training Objective

Stage 1: SFT warmup (single-teacher selection). We initialize the student π_S with supervised fine-tuning on a single teacher response per input. When multiple teacher responses are available in the dataset, we select one response per input: for closed-ended tasks, we select the response with the highest quality score q_k ; for open-ended tasks, we randomly select one response from the pool to avoid introducing bias from arbitrary selection criteria. We then apply standard autoregressive cross-entropy:

$$\mathcal{L}_{\text{SFT}} = -\log \pi_S(T_{\text{best}} | V, Q). \tag{5}$$

This stage provides stable initialization before adversarial training.

Stage 2: RL-based adversarial distillation with composite rewards. We optimize the student using policy-gradient RL on freshly sampled student rollouts with a composite reward that combines distribution-level and content-level signals. For each prompt, we sample N student responses $S_i \sim \pi_S(\cdot | V, Q)$, each paired with a teacher response $T_{m(i)}$ via task-adaptive matching. Eq. 6 decomposes the reward into four components:

$$R(S_i) = \alpha D_\phi(S_i) + \beta R_{\text{outer}}(S_i) + \eta R_{\text{task}}(S_i) + \delta R_{\text{content}}(S_i), \tag{6}$$

where the weights satisfy $\alpha + \beta + \eta + \delta = 1$ to maintain reward scale consistency, $D_\phi(S_i)$ is the discriminator score (higher values indicate more teacher-like outputs), R_{outer} encourages a valid outer response format, R_{task} checks task-specific answer formatting (e.g., timestamps / options / boxes), and R_{content} measures correctness for closed-ended tasks.

Reward specification. $R_{\text{outer}} \in \{0, 1\}$ indicates valid outer response format (1 if response contains valid tags including ‘<answer>’ and thinking tags like “); $R_{\text{task}} \in \{0, 1\}$ checks task-specific format compliance (e.g., temporal grounding with ‘<t>x</t>’ to ‘<t>x</t>’, MCQ option letters); $R_{\text{content}} \in [0, 1]$ is the GT-based quality score identical to q_k in Eq. 2 for closed-ended tasks (0 for open-ended). By separating format validity from content correctness, we align reward shaping with evaluation metrics rather than relying on brittle lexical overlap proxies.

3.5 Discriminator and Adversarial Training

Discriminator architecture. We implement the discriminator as a *critic-as-discriminator* that assigns a scalar score to a generated response. Concretely, we reuse the critic value head to score the last token of a response, yielding a single scalar per sequence. Higher scores indicate teacher-like responses.

Table 1: Main results on video and image QA benchmarks. Metrics follow official protocols (accuracy for QA and $\Delta_{\text{knowledge}}$ for Video-MMMU). **Frames** denotes test-time frames. Under the same 4B scale and frame budget, R-MSD outperforms both the base model and an original SFT+RL baseline.

Model	Frames	Video QA					Image QA	
		VideoMME	Video-MMMU	WorldSense	LongVideoBench	MLVU_MCQ	MathVista	MathVerse
<i>Proprietary Models</i>								
GPT-4o [Hurst et al., 2024]	-	71.9	61.2	-	66.7	-	63.8	41.2
Gemini-2.5-Pro [Comanici et al., 2025]	-	84.3	83.6	-	77.6	-	82.7	-
Seed1.5-VL [Guo et al., 2025b]	-	77.9	81.4	-	74.0	82.1	85.6	-
<i>2B-Scale Open Models</i>								
InternVL2.5-2B [Chen et al., 2024c]	-	51.9	-	-	52.0	61.4	51.3	30.6
InternVL3-2B [Zhu et al., 2025b]	-	58.9	-	-	55.4	64.2	57.0	25.3
InternVL3.5-2B [Wang et al., 2025]	-	58.4	-	-	57.4	64.4	71.8	53.4
VideoLLaMA3-2B [Zhang et al., 2025]	-	59.6	-	-	57.1	65.4	59.2	-
Qwen3-VL-2B-Instruct [Bai et al., 2025a]	64	60.8	39.5	42.6	53.6	66.8	58.9	51.1
<i>4B-Scale Open Models</i>								
InternVL2.5-4B [Chen et al., 2024c]	-	62.3	-	-	55.2	68.3	60.5	37.1
InternVL3.5-4B [Wang et al., 2025]	-	65.4	-	-	60.8	70.4	77.1	61.7
Qwen3-VL-4B-Instruct [Bai et al., 2025a]	64	63.8	55.4	46.7	59.3	72.4	69.5	45.7
Original SFT+RL (4B)	64	64.0	55.9	46.3	57.2	73.1	71.2	46.8
<i>7B-8B-Scale Open Models</i>								
InternVL2.5-8B [Chen et al., 2024c]	-	64.2	-	-	60.0	68.9	64.4	39.5
InternVL3-8B [Zhu et al., 2025b]	-	66.3	-	-	58.8	71.4	71.6	39.8
InternVL3.5-8B [Wang et al., 2025]	-	66.0	-	-	62.5	70.2	78.4	61.5
VideoLLaMA3-7B [Zhang et al., 2025]	-	66.2	-	-	59.8	44.1	67.1	-
Qwen3-VL-8B-Instruct [Bai et al., 2025a]	64	64.0	63.3	-	61.5	75.1	74.2	58.1
<i>Ours</i>								
Ours (2B)	64	61.9	40.8	45.7	53.7	68.2	61.4	55.3
Ours (4B)	64	65.3	58.6	49.2	58.8	73.2	72.1	49.3

Discriminator loss. Given a matched student–teacher pair $(S_i, T_{m(i)})$, the discriminator is trained with the quality-weighted GAD pairwise objective:

$$\mathcal{L}_D = \mathbb{E}_i \left[q_{m(i)} \cdot -\log \sigma \left(D_\phi(T_{m(i)}) - D_\phi(S_i) \right) \right], \quad (7)$$

where σ is the sigmoid function and $q_{m(i)}$ is the quality score of teacher response $T_{m(i)}$ (Eq. 2). Task-adaptive quality weighting enters through the matching distribution $m(i)$ (closed-ended tasks preferentially pair higher-quality teachers), rather than via an explicit per-sample weight inside \mathcal{L}_D .

Student RL objective. The student is trained to maximize the composite reward from Eq. 6. Using the policy gradient formulation, the complete Stage 2 objective is:

$$\mathcal{L}_{\text{RL}} = -\mathbb{E}_{S \sim \pi_S} [R(S)] + \gamma D_{\text{KL}}(\pi_S \| \pi_{\text{ref}}), \quad (8)$$

where $R(S)$ is the composite reward from Eq. 6 and the KL penalty term prevents the policy from deviating too far from a reference policy (initialized from Stage 1). The adversarial component corresponds to the discriminator term in $R(S)$, which encourages the student to produce outputs that receive high discriminator scores (i.e., teacher-like outputs).

3.6 Complexity and Practical Considerations

Relative to single-sample distillation, our method introduces additional teacher sampling cost proportional to K . In exchange, training uses richer supervision without changing the inference-time architecture. Thus, the additional cost is paid only during distillation training. In practice, K controls a direct quality–cost trade-off, which we quantify in the sensitivity study in Table 4.

4 Experiments

We design experiments to evaluate three claims from section 1: (1) R-MSD improves over single-sample baselines under matched budgets, (2) each component contributes to the final gain, and (3) teacher sampling variance is a practical bottleneck. The section is organized accordingly: subsection 4.2 focuses on Claim 1, subsection 4.3 examines Claim 2, and subsection 4.4 provides dedicated evidence for Claim 3.

Table 2: Results on V-STaR [Cheng et al., 2025]. We report When (temporal IoU) and Where (visual IoU) under the official evaluation. **Frames** denotes test-time frames. Improvements indicate better spatio-temporal grounding under teacher sampling variance.

Model	Frames	When (Temporal IoU)		Where (Visual IoU)	
		Chain1	Chain2	Chain1	Chain2
GPT-4o [Hurst et al., 2024]	-	16.7	12.8	6.5	3.0
Gemini-2-Flash [Comanici et al., 2025]	-	24.5	23.8	4.6	2.2
Video-LLaMA3 [Zhang et al., 2025]	-	23.0	23.1	0.9	0.2
LLaVA-Video [Zhang et al., 2024]	-	10.5	12.2	1.9	1.3
VideoChat2 [Li et al., 2024b]	-	13.7	12.5	2.5	1.0
Oryx-1.5-7B [Liu et al., 2024]	-	13.5	14.8	10.1	3.5
InternVL-2.5-8B [Chen et al., 2024c]	-	8.7	7.8	0.7	0.1
Qwen2.5-VL-7B [Bai et al., 2025b]	-	15.4	13.8	17.0	2.5
TRACE [Guo et al., 2024]	-	19.1	17.1	0.0	0.0
Sa2VA-8B [Yuan et al., 2025]	-	0.1	0.0	32.3	37.5
Open-o3 Video [Meng et al., 2025]	-	24.5	24.0	25.4	6.0
Qwen3-VL-4B [Bai et al., 2025a]	64	21.3	18.5	22.3	5.0
Ours (4B)	64	25.2	23.4	24.8	7.0

4.1 Experimental Setup

4.1.1 Benchmarks

We evaluate on six public video understanding benchmarks : VideoMME, Video-MMMU, WorldSense, LongVideoBench, MLVU_MCQ, and VsTAR [Cheng et al., 2025], plus two image QA benchmarks (MathVista, MathVerse) for cross-domain evaluation. All benchmarks use official evaluation splits and metrics. VideoMME, WorldSense, LongVideoBench, and MLVU_MCQ use multiple-choice accuracy; Video-MMMU uses the knowledge-gain metric $\Delta_{\text{knowledge}}$; VsTAR uses grounding metrics (tIoU/IoU); MathVista and MathVerse use accuracy. With one exception (VsTAR, evaluated via tIoU/IoU), all benchmarks are treated as closed-ended tasks with exact-match evaluation.

4.1.2 Training data

We construct our distillation dataset from VideoR1 [Feng et al., 2025] (10% subset) and OpenO3 [Meng et al., 2025] (full dataset). The frozen Qwen3-VL-235B teacher processes raw video-question pairs to generate supervision annotations. Stage 1 SFT warmup uses 50K samples; Stage 2 RL-based adversarial distillation optimization uses 60K samples with multi-sample quality signals. All training samples are disjoint from evaluation benchmarks.

4.1.3 Models and training protocol

We use a frozen Qwen3-VL-235B teacher and Qwen3-VL-4B student under black-box distillation. We set teacher pool size $K=4$, sample $N=8$ student rollouts per input during Stage 2, and train for 1 epoch per stage. Optimization uses AdamW (learning rate 2×10^{-6} for student, 1×10^{-6} for discriminator) with batch size 128. The reward weights are $(\alpha, \beta, \eta, \delta) = (0.4, 0.1, 0.1, 0.4)$. Students train with 16 frames per video and are evaluated with 64 frames at test time.

4.2 Main Results

After introducing the setup, we first evaluate Claim 1 by comparing our distilled 4B student with existing video LVLMs on the full suite of six video benchmarks, and also examines cross-domain transfer on two image QA benchmarks. All evaluations use each benchmark’s official split and metric.

Compared models. We compare against publicly available video LVLMs at similar scale. Larger models are included only as context, not direct baselines. Our 4B student is distilled from a larger frozen teacher using R-MSD (section 3), and prior-work numbers use official checkpoints/scripts when available. We additionally report an in-house *original SFT+RL* 4B baseline under the same teacher, student scale, training budget, and frame budget for direct protocol comparison.

Table 3: Core component ablation on VideoMME and Video-MMMU (accuracy, %). K : teacher sample count. “Filter” applies threshold τ to remove low-quality teacher samples ($q_k < \tau$). “Weight” enables quality-weighted discriminator updates by q_k . Setting A reports Stage 1 single-sample SFT; vanilla Qwen3-VL-4B is in Table 1.

Setting	K	Filter	Weight	VideoMME	Video-MMMU
A (single-sample)	1	No	No	63.8	54.4
B (multi-sample)	4	No	No	64.5	55.9
C (+filtering)	4	Yes	No	65.0	57.2
D (ours)	4	Yes	Yes	65.3	58.6

Table 4: Sensitivity analyses for teacher sample count K (left; VideoMME/Video-MMMU accuracy, %) and quality threshold τ (right; valid-sample ratio and accuracy) under the full method. We select $\tau = 0.3$ to balance low-quality removal (72% retention) and teacher-pool diversity.

K	VideoMME	Video-MMMU	τ	Valid-sample ratio	VideoMME	Video-MMMU
2	64.8	57.1	0.0	100%	64.5	55.9
4	65.3	58.6	0.2	87%	65.0	58.1
8	65.5	58.9	0.3	72%	65.3	58.6
			0.5	45%	64.8	57.2

Results. Table 1 summarizes five video QA and two image QA benchmarks; Table 2 reports VsTAR separately. Under the same 64-frame test budget, our 4B student consistently outperforms Qwen3-VL-4B. Gains range from +0.8 (MLVU) to +3.6 (MathVerse), with VideoMME (+1.5), Video-MMMU (+3.2), WorldSense (+2.5), and MathVista (+2.6); LongVideoBench shows no significant change. On VsTAR (Table 2), our 4B student also improves on all four chains, with Chain2 temporal IoU (+4.9) and Chain2 visual IoU (+2.0).

Interpretation. Consistent improvements confirm R-MSD enhances supervision reliability; non-uniform gains align with teacher sampling variance across tasks.

4.3 Ablation and Analysis

This subsection evaluates Claim 2 by dissecting which components of R-MSD are responsible for the gains beyond multi-sample training and how sensitive the method is to the number and quality of teacher samples.

4.3.1 Core component ablation

We compare four settings to isolate gains beyond naive multi-sample training: A ($K=1$), B ($K=4$), C (+filtering, $\tau=0.3$), and D (+weighting). Except A, all settings use $K=4$ with the same teacher, student, and training schedule. **Filtering** removes low-quality teacher samples ($q_k < \tau$) for closed-ended tasks. **Weighting** trains the discriminator with quality weights, giving more influence to higher-quality teacher responses. Table 3 reports results on VideoMME and Video-MMMU.

4.3.2 Sensitivity to sample count K

Table 4 (left) shows that increasing K from 1 to 4 improves both benchmarks, while $K=8$ yields only marginal extra gain.

4.3.3 Sensitivity to quality threshold τ

Table 4 (right) shows that moderate filtering ($\tau=0.2$ or 0.3) improves both VideoMME and Video-MMMU, whereas aggressive filtering ($\tau=0.5$) removes too many samples and slightly hurts performance. This supports discarding clearly low-quality teacher responses while preserving teacher-pool diversity.

Table 5: Task-adaptive strategy validation: average accuracy (%) over closed-ended and open-ended task subsets across VideoMME and Video-MMMU under GT-based scoring vs. uniform weighting.

Task family	GT-based scoring	Uniform weighting
Closed-ended tasks	57.8	56.2
Open-ended tasks	58.4	59.1

4.3.4 Pass@k on Video-MMMU

Following recent work on evaluating reasoning capability boundaries [Yue et al., 2025], we use Pass@ k to measure reliability under repeated decoding: for each Video-MMMU query, we sample k responses with $T=1.0$ and top- $p=0.9$, counting a success if any response matches the ground-truth option. Unlike pass@1 which reflects average-case behavior, pass@ k at large values reveals a model’s problem-solving potential [Yue et al., 2025].

Figure 3 (right) shows the Pass@ k curve from $k=1$ to $k=128$. Our method achieves +3.2% higher Pass@1 than Qwen3-VL-4B while converging to a similar upper bound, indicating R-MSD primarily improves the probability of correct answers with fewer inference calls.

4.3.5 Task-adaptive strategy validation

Table 5 compares GT-based scoring versus uniform weighting across closed-ended and open-ended task subsets.

For closed-ended tasks, GT-based scoring outperforms uniform weighting, while for open-ended tasks the trend reverses. This supports our task-adaptive design: lexical metrics for open-ended responses can hurt performance.

Reproducibility. We follow official benchmark evaluation scripts; when prior work lacks frame counts or evaluation details, we retain published numbers as context without direct fairness claims beyond matched settings.

4.4 Teacher Sampling Variance Analysis

The main results in subsection 4.2 show that R-MSD achieves consistent improvements across benchmarks, but with non-uniform gain patterns (e.g., +3.2 on Video-MMMU vs. +0.8 on MLVU_MCQ). To understand why improvements vary by task, we analyze teacher sampling variance and examine how it relates to the performance gains we observe.

We analyze 200 teacher responses from a frozen Qwen3-VL-235B teacher across 8 task types. Figure 3 summarizes per-task quality distributions and Pass@ k behavior.

Cross-question variance is substantial: quality ranges from 0.10 to 1.0 ($\mu=0.75$, $\sigma=0.22$). MCQ shows high stability ($\mu=0.96$, $\sigma=0.10$), while visual QA exhibits higher variance ($\mu=0.64$, $\sigma=0.24$). Within-question sampling variance is also significant: σ_{sampling} ranges from 0.07 (MCQ) to 0.15 (visual QA), with quality spans of [0.50, 0.85] for OCR and [0.65, 1.00] for numerical tasks. Format violations occur in 1% of samples overall (10% for temporal QA).

These trends explain the gains: high-variance tasks such as Video-MMMU (+3.2) benefit most from R-MSD, whereas LongVideoBench shows little improvement due to a frame-count mismatch (training uses 16 frames despite its longer-context demands).

5 Conclusion

We study teacher decoding uncertainty as a practical bottleneck in video LVLm distillation. Through empirical analysis, we identify two variance dimensions: **(1)** cross-question variance ($\sigma=0.22$ globally) where different questions yield different teacher quality; and **(2)** within-question decoding uncertainty ($\sigma_{\text{sampling}}\approx 0.10$ on average) where repeated samples of the same question span quality ranges of [0.50, 0.85] for OCR and [0.65, 1.00] for numerical tasks. Combined with format violations (1.0% overall, about 10% for temporal QA), this makes single-sample supervision fundamentally unreliable.

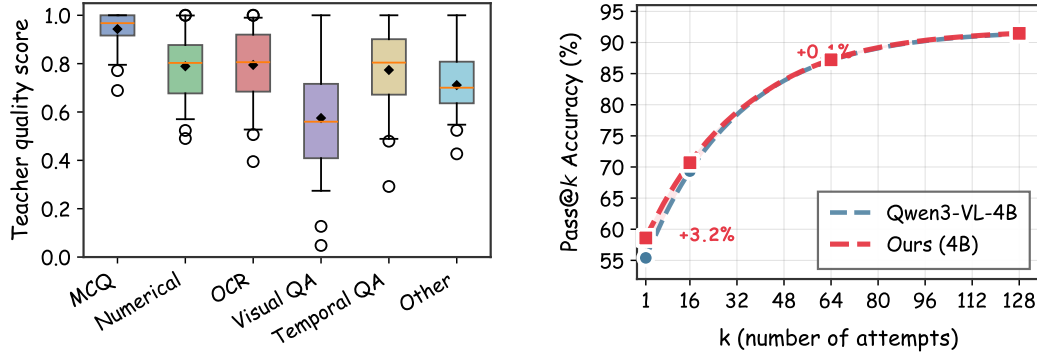


Figure 3: Per-task teacher variance and Pass@ k behavior on Video-MMMU. **Left:** Teacher quality distribution by task type; box plots over 200 teacher responses across six task families highlight that high-stability closed-ended tasks (e.g., MCQ, numerical) have lower variance, while higher-variance tasks such as visual QA exhibit wider spreads. **Right:** Pass@ k accuracy on Video-MMMU as a function of k (number of sampled student responses per query); our method achieves +3.2% higher Pass@1 accuracy than Qwen3-VL-4B while converging to a similar upper bound as k increases.

To address this, we propose R-MSD (Reliable Multi-Sample Distillation), which samples a teacher pool per input and applies task-adaptive matching: for closed-ended tasks, it preferentially pairs student rollouts with higher-quality teacher responses measured against ground truth; for open-ended tasks, it uses uniform pairing to avoid brittle lexical bias. Building on this matching strategy, we first perform SFT warmup and then apply RL-based adversarial distillation, where an online discriminator provides distribution-level alignment signals.

Across six video benchmarks and two image QA benchmarks, R-MSD consistently outperforms single-sample and uniform multi-sample baselines under matched training budgets, with gains of +1.5 on VideoMME, +3.2 on Video-MMMU, and +3.6 on MathVerse. Under the same protocol, an original SFT+RL 4B baseline shows only marginal improvement, further highlighting the benefit of task-adaptive multi-sample supervision.

Summary. Our findings show that supervision *selection strategy* is as important as supervision quantity in response-based video distillation. For closed-ended tasks, quality-biased pairing improves performance by filtering low-quality teacher samples; for open-ended tasks, uniform pairing preserves semantic diversity and avoids brittle lexical penalties. This task-adaptive paradigm improves distillation reliability without extra reward models or complex infrastructure.

Limitations. Our closed-ended task quality scoring relies on task-specific ground-truth annotations and may not directly apply in weakly supervised settings. For open-ended tasks, uniform weighting is a conservative choice that preserves semantic diversity but does not explicitly rank semantic correctness. The multi-sample protocol increases training-time compute approximately proportional to K .

Future work. Future work includes semantic quality estimators for open-ended responses, adaptive selection of K based on input difficulty, and integration with other distillation/alignment objectives. Reference-aware reward correction in strong-to-weak settings is another promising direction for improving quality-signal fidelity when teacher and student capacities differ substantially.

References

- Yukang Chen, Fuzhao Xue, Dacheng Li, Qinghao Hu, Ligeng Zhu, Xiuyu Li, Yunhao Fang, Haotian Tang, Shang Yang, Zhijian Liu, et al. Longvila: Scaling long-context visual language models for long videos. *arXiv preprint arXiv:2408.10188*, 2024a.
- Zeqian Li, Shangzhe Di, Zhonghua Zhai, Weilin Huang, Yanfeng Wang, and Weidi Xie. Universal video temporal grounding with generative multi-modal large language models. *arXiv preprint arXiv:2506.18883*, 2025a.

- Yongxin Guo, Jingyu Liu, Mingda Li, Dingxin Cheng, Xiaoying Tang, Dianbo Sui, Qingbin Liu, Xi Chen, and Kevin Zhao. Vtg-llm: Integrating timestamp knowledge into video llms for enhanced video temporal grounding. In *Proceedings of the AAAI Conference on Artificial Intelligence*, volume 39, pages 3302–3310, 2025a.
- Geoffrey Hinton, Oriol Vinyals, and Jeff Dean. Distilling the knowledge in a neural network. *arXiv preprint arXiv:1503.02531*, 2015.
- Yang Yue, Zhiqi Chen, Rui Lu, Andrew Zhao, Zhaokai Wang, Shiji Song, and Gao Huang. Does reinforcement learning really incentivize reasoning capacity in llms beyond the base model? *arXiv preprint arXiv:2504.13837*, 2025.
- Shan You, Chang Xu, Chao Xu, and Dacheng Tao. Learning from multiple teacher networks. In *Proceedings of the 23rd ACM SIGKDD international conference on knowledge discovery and data mining*, pages 1285–1294, 2017.
- Amir M Mansourian, Amir Mohammad Babaei, and Shohreh Kasaei. Enriching knowledge distillation with cross-modal teacher fusion. *arXiv preprint arXiv:2511.09286*, 2025.
- Tianzhu Ye, Li Dong, Zewen Chi, Xun Wu, Shaohan Huang, and Furu Wei. Black-box on-policy distillation of large language models. *arXiv preprint arXiv:2511.10643*, 2025.
- Yoon Kim and Alexander M Rush. Sequence-level knowledge distillation. In *Proceedings of the 2016 conference on empirical methods in natural language processing*, pages 1317–1327, 2016.
- Shihan Dou, Shichun Liu, Yuming Yang, Yicheng Zou, Yunhua Zhou, Shuhao Xing, Chenhao Huang, Qiming Ge, Demin Song, Haijun Lv, et al. Pre-trained policy discriminators are general reward models. *arXiv preprint arXiv:2507.05197*, 2025.
- KunChang Li, Yinan He, Yi Wang, Yizhuo Li, Wenhai Wang, Ping Luo, Yali Wang, Limin Wang, and Yu Qiao. Videochat: Chat-centric video understanding. *Science China Information Sciences*, 68(10):200102, 2025b.
- Muhammad Maaz, Hanoona Rasheed, Salman Khan, and Fahad Khan. Video-chatgpt: Towards detailed video understanding via large vision and language models. In *Proceedings of the 62nd Annual Meeting of the Association for Computational Linguistics (Volume 1: Long Papers)*, pages 12585–12602, 2024.
- Bin Lin, Yang Ye, Bin Zhu, Jiayi Cui, Munan Ning, Peng Jin, and Li Yuan. Video-llava: Learning united visual representation by alignment before projection. In *Proceedings of the 2024 conference on empirical methods in natural language processing*, pages 5971–5984, 2024.
- Yanwei Li, Chengyao Wang, and Jiaya Jia. Llama-vid: An image is worth 2 tokens in large language models. In *European Conference on Computer Vision*, pages 323–340. Springer, 2024a.
- Lin Xu, Yilin Zhao, Daquan Zhou, Zhijie Lin, See Kiong Ng, and Jiashi Feng. Pllava: Parameter-free llava extension from images to videos for video dense captioning. *arXiv preprint arXiv:2404.16994*, 2024.
- Yuanhan Zhang, Jinming Wu, Wei Li, Bo Li, Zejun Ma, Ziwei Liu, and Chunyuan Li. Llava-video: Video instruction tuning with synthetic data. *arXiv preprint arXiv:2410.02713*, 2024.
- Lin Chen, Xilin Wei, Jinsong Li, Xiaoyi Dong, Pan Zhang, Yuhang Zang, Zehui Chen, Haodong Duan, Zhenyu Tang, Li Yuan, et al. Sharegpt4video: Improving video understanding and generation with better captions. *Advances in Neural Information Processing Systems*, 37:19472–19495, 2024b.
- Long Ouyang, Jeffrey Wu, Xu Jiang, Diogo Almeida, Carroll Wainwright, Pamela Mishkin, Chong Zhang, Sandhini Agarwal, Katarina Slama, Alex Ray, et al. Training language models to follow instructions with human feedback. *Advances in neural information processing systems*, 35:27730–27744, 2022.
- Rafael Rafailov, Archit Sharma, Eric Mitchell, Christopher D Manning, Stefano Ermon, and Chelsea Finn. Direct preference optimization: Your language model is secretly a reward model. volume 36, pages 53728–53741, 2023.

- Yufei Wang, Zhanyi Sun, Jesse Zhang, Zhou Xian, Erdem Biyik, David Held, and Zackory Erickson. RL-vlm-f: Reinforcement learning from vision language foundation model feedback. *arXiv preprint arXiv:2402.03681*, 2024.
- Ke Zhu, Yu Wang, Yanpeng Sun, Qiang Chen, Jiangjiang Liu, Gang Zhang, and Jingdong Wang. Continual sft matches multimodal rlhf with negative supervision. In *Proceedings of the Computer Vision and Pattern Recognition Conference*, pages 14615–14624, 2025a.
- Leo Gao, John Schulman, and Jacob Hilton. Scaling laws for reward model overoptimization. In *International Conference on Machine Learning*, pages 10835–10866. PMLR, 2023.
- Wenkai Yang, Weijie Liu, Ruobing Xie, Kai Yang, Saiyong Yang, and Yankai Lin. Learning beyond teacher: Generalized on-policy distillation with reward extrapolation. *arXiv preprint arXiv:2602.12125*, 2026.
- Chaofei Wang, Shaowei Zhang, Shiji Song, and Gao Huang. Learn from the past: Experience ensemble knowledge distillation. In *2022 26th International Conference on Pattern Recognition (ICPR)*, pages 4736–4743. IEEE, 2022.
- Chunting Zhou, Pengfei Liu, Puxin Xu, Srinivasan Iyer, Jiao Sun, Yuning Mao, Xuezhe Ma, Avia Efrat, Ping Yu, Lili Yu, et al. Lima: Less is more for alignment. *Advances in Neural Information Processing Systems*, 36:55006–55021, 2023.
- Hanze Dong, Wei Xiong, Deepanshu Goyal, Yihan Zhang, Winnie Chow, Rui Pan, Shizhe Diao, Jipeng Zhang, Kashun Shum, and Tong Zhang. Raft: Reward ranked finetuning for generative foundation model alignment. *arXiv preprint arXiv:2304.06767*, 2023.
- Takashi Fukuda, Masayuki Suzuki, Gakuto Kurata, Samuel Thomas, Jia Cui, and Bhuvana Ramabhadran. Efficient knowledge distillation from an ensemble of teachers. In *Interspeech*, pages 3697–3701, 2017.
- Aaron Hurst, Adam Lerer, Adam P Goucher, Adam Perelman, Aditya Ramesh, Aidan Clark, AJ Ostrow, Akila Welihinda, Alan Hayes, Alec Radford, et al. Gpt-4o system card. *arXiv preprint arXiv:2410.21276*, 2024.
- Gheorghe Comanici, Eric Bieber, Mike Schaekermann, Ice Pasupat, Noveen Sachdeva, Inderjit Dhillon, Marcel Blistein, Ori Ram, Dan Zhang, Evan Rosen, et al. Gemini 2.5: Pushing the frontier with advanced reasoning, multimodality, long context, and next generation agentic capabilities. *arXiv preprint arXiv:2507.06261*, 2025.
- Dong Guo, Faming Wu, Feida Zhu, Fuxing Leng, Guang Shi, Haobin Chen, Haoqi Fan, Jian Wang, Jianyu Jiang, Jiawei Wang, et al. Seed1. 5-vl technical report. *arXiv preprint arXiv:2505.07062*, 2025b.
- Zhe Chen, Weiyun Wang, Yue Cao, Yangzhou Liu, Zhangwei Gao, Erfei Cui, Jinguo Zhu, Shenglong Ye, Hao Tian, Zhaoyang Liu, et al. Expanding performance boundaries of open-source multimodal models with model, data, and test-time scaling. *arXiv preprint arXiv:2412.05271*, 2024c.
- Jinguo Zhu, Weiyun Wang, Zhe Chen, Zhaoyang Liu, Shenglong Ye, Lixin Gu, Hao Tian, Yuchen Duan, Weijie Su, Jie Shao, et al. Internvl3: Exploring advanced training and test-time recipes for open-source multimodal models. *arXiv preprint arXiv:2504.10479*, 2025b.
- Weiyun Wang, Zhangwei Gao, Lixin Gu, Hengjun Pu, Long Cui, Xingguang Wei, Zhaoyang Liu, Linglin Jing, Shenglong Ye, Jie Shao, et al. Internvl3. 5: Advancing open-source multimodal models in versatility, reasoning, and efficiency. *arXiv preprint arXiv:2508.18265*, 2025.
- Boqiang Zhang, Kehan Li, Zesen Cheng, Zhiqiang Hu, Yuqian Yuan, Guanzheng Chen, Sicong Leng, Yuming Jiang, Hang Zhang, Xin Li, et al. Videollama 3: Frontier multimodal foundation models for image and video understanding. *arXiv preprint arXiv:2501.13106*, 2025.
- Shuai Bai, Yuxuan Cai, Ruizhe Chen, Keqin Chen, Xionghui Chen, Zesen Cheng, Lianghao Deng, Wei Ding, Chang Gao, Chunjiang Ge, et al. Qwen3-vl technical report. *arXiv preprint arXiv:2511.21631*, 2025a.

- Zixu Cheng, Jian Hu, Ziquan Liu, Chenyang Si, Wei Li, and Shaogang Gong. V-star: Benchmarking video-llms on video spatio-temporal reasoning. *arXiv preprint arXiv:2503.11495*, 2025.
- Kunchang Li, Yali Wang, Yinan He, Yizhuo Li, Yi Wang, Yi Liu, Zun Wang, Jilan Xu, Guo Chen, Ping Luo, et al. Mvbench: A comprehensive multi-modal video understanding benchmark. In *Proceedings of the IEEE/CVF Conference on Computer Vision and Pattern Recognition*, pages 22195–22206, 2024b.
- Zuyan Liu, Yuhao Dong, Ziwei Liu, Winston Hu, Jiwen Lu, and Yongming Rao. Oryx mllm: On-demand spatial-temporal understanding at arbitrary resolution. *arXiv preprint arXiv:2409.12961*, 2024.
- Shuai Bai, Keqin Chen, Xuejing Liu, Jialin Wang, Wenbin Ge, Sibao Song, Kai Dang, Peng Wang, Shijie Wang, Jun Tang, Humen Zhong, Yanzhi Zhu, Mingkun Yang, Zhaohai Li, Jianqiang Wan, Pengfei Wang, Wei Ding, Zheren Fu, Yiheng Xu, Jiabo Ye, Xi Zhang, Tianbao Xie, Zesen Cheng, Hang Zhang, Zhibo Yang, Haiyang Xu, and Junyang Lin. Qwen2.5-vl technical report, 2025b. URL <https://arxiv.org/abs/2502.13923>.
- Yongxin Guo, Jingyu Liu, Mingda Li, Qingbin Liu, Xi Chen, and Xiaoying Tang. Trace: Temporal grounding video llm via causal event modeling. *arXiv preprint arXiv:2410.05643*, 2024.
- Haobo Yuan, Xiangtai Li, Tao Zhang, Yueyi Sun, Zilong Huang, Shilin Xu, Shunping Ji, Yunhai Tong, Lu Qi, Jiashi Feng, et al. Sa2va: Marrying sam2 with llava for dense grounded understanding of images and videos. *arXiv preprint arXiv:2501.04001*, 2025.
- Jiahao Meng, Xiangtai Li, Haochen Wang, Yue Tan, Tao Zhang, Lingdong Kong, Yunhai Tong, Anran Wang, Zhiyang Teng, Yujing Wang, et al. Open-o3 video: Grounded video reasoning with explicit spatio-temporal evidence. *arXiv preprint arXiv:2510.20579*, 2025.
- Kaituo Feng, Kaixiong Gong, Bohao Li, Zonghao Guo, Yibing Wang, Tianshuo Peng, Junfei Wu, Xiaoying Zhang, Benyou Wang, and Xiangyu Yue. Video-r1: Reinforcing video reasoning in mllms. *arXiv preprint arXiv:2503.21776*, 2025.